PCCP

One-electron redox kinetics of aqueous transition metal couples $Zn^{2+/+}$, $Co^{2+/+}$, and $Ni^{2+/+}$ using pulse radiolysis

Journal:	*Physical Chemistry Chemical Physics*
Manuscript ID	CP-ART-06-2020-003214.R1
Article Type:	Paper
Date Submitted by the Author:	24-Jul-2020
Complete List of Authors:	Lisovskaya, Alexandra; University of Notre Dame, Notre Dame Radiation Laboratory Kanjana, Kotchaphan; University of Notre Dame, Notre Dame Radiation Laboratory Bartels, D; University of Notre Dame, Notre Dame Radiation Laboratory

ARTICLE

One-electron redox kinetics of aqueous transition metal couples $Zn^{2+/+}$, $Co^{2+/+}$, and $Ni^{2+/+}$ using pulse radiolysis

Received 15th June 2020,
Accepted 00th July 2020

DOI: 10.1039/x0xx00000x

Alexandra Lisovskaya, Kotchaphan Kanjana† and David M. Bartels*

The one-electron redox potentials for aqueous metal couples $Co^{2+/+}$ and $Ni^{2+/+}$ have been investigated by pulse radiolysis using their reactions with a series of reference compounds to establish the most positive upper limits of E^0. Experiments with Zn^+ were also carried out to confirm the characteristic shape of expected reduction kinetics. Both formate ion and *t*-BuOH were employed to scavenge •OH radicals and •H atoms. Kinetics and fitted first and second order reaction rates are reported for reactions with methyl viologen, fluorescein, $Ru(NH_3)_6^{3+}$, $Co(en)_3^{2+}$, Co(sepulcrate)$^{3+}$, $Ru(bpy)_3^{2+}$, $Cr(bpy)_3^{3+}$, and $Ni(Me_6[14]4,11\text{-dieneN}_4)^{2+}$. Previous work demonstrated both Co^{2+} and Ni^{2+} can be reduced by $CO_2^{\bullet-}$ radical, giving a negative E^0 limit of -1.9 V *vs* SHE. A definite reaction of Ni^+ with fluorescein di-anion provides the new upper limit of the $Ni^{2+/+}$ couple as -0.906 V *vs* SHE. The reaction of Co^+ with $Ru(bpy)_3^{2+}$ has been confirmed giving E^0 = -1.3 V *vs* SHE as a rigorous upper limit of the $Co^{2+/+}$ couple. In the case of $Co^{2+/+}$, kinetics were complicated by a self-catalyzed metal clustering phenomenon. Initiation rate constants of this process are also reported.

Introduction

Monovalent first-row transition metal ions ($M^+_{(aq)}$) are short-lived species that can be produced from the reduction of $M^{2+}_{(aq)}$ by the hydrated electron.[1–3] The radiation chemistry of the reduced transition metal ions dissolved in the cooling water of nuclear reactors can substantially affect the complex process of corrosion and activity transport.[4,5] In a recent study we have measured the reduction reactions of these species with the hydrated electron up to high temperature.[3] The redox potentials (E^0) of a vast number of transition metal ions and their complexes have been studied and the refined values have been tabulated.[6–9] We were surprised to discover that the redox potentials of the aqueous divalent-to-monovalent first row transition metal couples have not been convincingly established, except for $Cu^{2+/+}$.[7] Direct electrochemical measurements of the redox potentials of these ions are not possible because the monovalent ions are transient species and do not live long enough in a liquid state.[10]

The room temperature radiation chemistry of the hyper-reduced $M^+_{(aq)}$ species was explored soon after the invention of the pulse radiolysis technique, and most of the early results are reviewed by Buxton and Sellers.[2] Co^{2+}, Ni^{2+} and Zn^{2+} can be reduced by the hydrated electron, E^0 = -2.87 V *vs* Standard Hydrogen Electrode (SHE), and observed by transient absorption spectroscopy.[2,11–19] The E^0 estimates for all of the first-row aqueous divalent cations were first made by Baxendale and Dixon [20] in 1964 using the gas phase electron affinity and a Born-theory approximation. These estimates suggest that E^0 should be -3.1 V for Fe^{2+} and Ni^{2+}, which is refuted by their ready reduction by the hydrated electron. Obviously the continuum Born theory omits any consideration of the metal d-orbitals and complexation, so this early calculation should not be taken seriously. The Marcus theory of electron transfer[21,22] was also used in an attempt to "triangulate" the reduction potentials of the metal ions from their reaction rates with other compounds of known reduction potential. [2,23] At that time it was not recognized that the pre-exponential factors of electron transfer reactions can vary dramatically due to the initial/final wave function overlap, so that the numbers derived from this method are also unreliable.[22]

In terms of direct observation of electron transfer reactions, no reactions between the $M^{2+/+}$ ions (M = Zn, Co, Ni) could be found to establish the correct order of their reduction potentials.[2] Reduction of the M^{2+} ions by $CO_2^{\bullet-}$ radical (E^0 = -1.90 V) is very slow ($k < 1\times10^5$ M^{-1} s^{-1}) when it occurs[19]. Buxton, *et al.*[24] reported convincing evidence from gamma radiolysis CO_2 product measurement, that $CO_2^{\bullet-}$ does reduce Ni^{2+} and Co^{2+}, but not Zn^{2+}. In 1994, Ershov *et al.*[17,18] reported that Ag^+ (E^0 = -1.8 V) and Tl^+ (E^0 = -1.9 V) can be reduced by Zn^+, which limits the redox potential for $Zn^{2+/+}$ to be more negative than -1.9 V. Katsumura and coworkers[16] attempted to observe a reaction of •H atoms (E^0 = -2.3V) with Zn^{2+} in strong acid but found none. Thus we have the possible redox potential range for the $Zn^{2+/+}$ couple as -1.9 V > E^0 > -2.87 V. Ershov, et al[17] have suggested that the reduction potential for Co^{2+}/Co^+ as well as for Cd^{2+}/Cd^+ should be very close to that of Ag^+/Ag^0 at -1.8±0.1 V. These authors demonstrated[17] using pulse radiolysis/transient absorption that

Notre Dame Radiation Laboratory, University of Notre Dame, Notre Dame, IN, 46556 USA.
†Present Address: Department of Chemistry, School of Science, Walailak University, Thasala, Nakhonsithammarat, 80160 Thailand.
*Corresponding Author: David.M.Bartels.5@nd.edu; phone (574) 631-5561; fax: (574) 631-8068; ORCID: 0000-0003-0552-3110.
Electronic Supplementary Information (ESI) available: [details of any supplementary information available should be included here]. See DOI: 10.1039/x0xx00000x

dimers $(CoAg)^{2+}$ or $(CdAg)^{2+}$ will form, and then react with Ag^+ ions to reform Co^{2+} or Cd^{2+} and the more stable Ag_2^+ dimer. More recently, the redox potential of $Ni^{2+/+}$ in water was calculated using a combination of quasi-chemical theory and ab initio molecular dynamics thermodynamic integration methods to be -1.05 or -1.28 V *vs* SHE.[25]

While rigorous negative limits for these three reduction potentials have been reported, there has been no experimental exploration of upper bounds for the Ni^{2+} and Co^{2+} reduction potentials. In this study, to reduce the possible range of values of E^0 we selected a group of reference compounds, whose redox potentials have been well studied, to react with the aqueous metal ions of interest. Pulse radiolysis/kinetics measurements were used to investigate upper limits of E^0 for $Co^{2+/+}$ and $Ni^{2+/+}$ metal couples under study. A full description of the kinetics measurements is reported below.

Experimental

The pulse radiolysis experiments were performed using an 8 MeV Linear Accelerator (LINAC) at the Notre Dame Radiation Laboratory. A monochromator/photomultiplier detection system with a 150W or 1kW pulsed xenon light source was initially employed for the UV-visible transient absorption measurements at short times (nanosecond to millisecond). The long time (>millisecond) measurements were carried out using a photodiode/filter wheel detection system with a very stable 4W "white" LED light source. The measured quantity is ΔOD, abbreviated in the figures below as OD (or mOD), which may include a "negative" bleach component.

In experiments with a more complex absorption spectrum, a recently-constructed multichannel detection system was used, which allows one to measure the absorption vs time over a full spectrum. The xenon lamp analyzing light is dispersed by a Acton SP2300 f/3.9 30cm imaging spectrograph onto an array of twenty-four 50cm length UV-transmitting fiber optic bundles. Each bundle is shaped at the spectrograph end into a rectangle of approximately 1.1 mm width x 3mm height. Depending on grating selection, the resolution (determined by the 1.1mm fiber "slit width") is approximately 6, 12, or 24 nm per channel, and the center of the spectrum is set by the spectrograph. Each of the twenty-four fiber bundles is terminated at the surface of a 2mm diameter biased Si photodiode (UVG50, -100V bias). Each photodiode is directly coupled to a home-built programmable two-stage operational amplifier assembly of 500MHz bandwidth. All photodiode channels can be switched (simultaneously) between 100 ohm or 3000 ohm load resistance. The former is useful for pulsed analyzing lamp and short timescales (ca. 1ns risetime), while the higher impedance is useful for long timescales (ca. 30ns risetime) without pulsing the lamp. The amplifier stages of each channel can be individually switched between 3.3, 10, 33, or 100x gain under computer control to provide an optimal light signal voltage between 0.1 and 1.0 V for the oscilloscope digitizers. Six 4-channel 8-bit 350MHz digital oscilloscopes (Tektronix TDS5034), triggered on the auxiliary triggers, are used to collect data in the hi-res mode, with minimum sampling period of 0.8ns/sample. The oscilloscope amplifier offsets and full scale are adjusted to optimize the digitizer "window" for best vertical resolution of a given transient. Commands to the oscilloscopes and transfer of data to a controlling computer is accomplished via ethernet using the VISA protocol. The absorption experiment has no separate I_o channel, so interleaved pairs of current-pulsed lamp trace sets with (I_t) and without (I_o) the radiolysis pulse are averaged and ratioed to obtain the transient absorption vs. time. Repetition rate of the experiment is limited to approximately 0.3-0.5Hz by the recovery time of the pulsed lamp. (Long experience shows that best S/N is obtained by waiting for full lamp recovery to obtain identical I_t and I_o lamp traces, rather than increasing the repetition rate.) In experiments where dark traces are desired for noise and Cerenkov light subtraction, these can be interleaved between the lamp pulses.

All metal ions (Co^{2+}, Ni^{2+} and Zn^{2+}) were purchased in the form of perchlorate salts (99.99 %, American Elements) and used without further purification. The solutions were all prepared using deionized water from the Serv-A-Pure Co. with 18 MΩ cm resistivity (organic carbon (CO_2) < 5 ppb). The reference compounds were methyl viologen dichloride hydrate (MV^{2+}, Sigma-Aldrich), fluorescein (high purity sodium salt, Amresco) and the chloride salts of the following ions, hexaammine ruthenium(III) ($Ru(NH_3)_6^{3+}$, Strem), tris(ethylenediamine) cobalt(III) ($Co(en)_3^{2+}$, Johnson Matthey), cobalt(III) sepulchrate ($Co(sep)^{3+}$, Aldrich), tris(2,2'-bipyridyl) ruthenium(II) ($Ru(bpy)_3^{2+}$, Strem). Tris(2,2'-bipyridyl) chromium(III) chloride ($Cr(bpy)_3^{3+}$) and [Ni(Me_6[14]4,11-dieneN$_4$)]$(ClO_4)_2$ (NMD^{2+}) were synthesized and purified according to the procedures reported previously.[26–28] Sodium formate (10mM, 99.998%, Sigma-Aldrich), tert-butyl alcohol and isopropyl alcohol (0.1 M, anhydrous ≥ 99.5 %, Sigma-Aldrich) were used as $^{\bullet}OH$ radical scavenger. The pH was adjusted using $HClO_4$ (0.03 mM, ACS Plus, Fisher Scientific). The reference compounds were selected based on their redox potentials and the reliability of the values. The initial absorption of the hydrated electron at 720 nm in pure degassed water, and the final absorption of $MV^{\bullet+}$ radical at 600nm in methyl viologen (MV^{2+}) solutions, were first used as the dosimeters in this study. A kinetics model with time-dependent spur decay rates and homogeneous chemistry from a delta-pulse, convolved with the rise time of the detector and the LINAC pulse width, was applied to obtain the e_{aq}^- concentration. Fitting the methyl viologen "blank" (no metal ions) with an appropriate simple kinetics model allows us to back out the initial yield of radicals. This kinetics model is described in detail in the Results and Discussion section. Eventually 10 mM KSCN solutions saturated with N_2O were also used for dosimetry at 475nm. Radiation chemical yield of $(SCN)_2^{\bullet-}$ is considered equal to $(5.2\pm0.05)\times10^{-4}$ m^2J^{-1} with ε=7580 $M^{-1}cm^{-1}$.[29]

Results and discussion

The oxidation-reduction reactions were studied by analyzing the absorption signals from reduced reference compounds A^{m-1} and/or from monovalent metal ions (M^+). The divalent metal ion

(M^{2+}) reacts with the hydrated electron e^-_{aq} producing the corresponding M^+ (1). In the presence of a reference compound A^m, the M^+ ion may reduce A^m giving a product in a reduced form A^{m-1} (2). The reduced A^{m-1} species were also generated from the reaction of the reference compound A^m with the hydrated electron (3), that were then oxidized by the M^{2+} ion (4). In some systems, the reduced forms of the metal ions and the acceptor compounds may undergo disproportionation reactions, as presented in reactions (5) and (6). The lists of the reference compounds used, with their redox potentials and the metal ion couple reactants are provided in Table 1.

$$e^-_{aq} + M^{2+} \rightarrow M^+ \quad (1)$$
$$A^m + M^+ \rightarrow A^{m-1} + M^{2+} \quad (2)$$
$$A^m + e^-_{aq} \rightarrow A^{m-1} \quad (3)$$
$$A^{m-1} + M^{2+} \rightarrow A^m + M^+ \quad (4)$$
$$M^+ + M^+ \rightarrow M^0 + M^{2+} \quad (5)$$
$$A^{m-1} + A^{m-1} \rightarrow \text{product} \quad (6)$$

The reference compounds $Ru(NH_3)_6^{3+}$, $Co(en)_3^{3+}$, $Cr(bpy)_3^{3+}$ and $Co(sep)^{3+}$ have relatively positive redox potentials (E^0 from +0.05 to -0.3 V).[8,26,30] Therefore, it was expected that they would be reduced by all three of the monovalent transition metal ions generated in reaction (1). In the systems with $Ru(NH_3)_6^{3+}$, $Co(en)_3^{3+}$ and $Co(sep)^{3+}$ the kinetics were investigated by following the decay of M^+ absorption.[2] In the case of $Cr(bpy)_3^{3+}$, the reduction by M^+ produces $Cr(bpy)_3^{2+}$ which strongly absorbs light at 560 nm.[37] The growth of the $Cr(bpy)_3^{2+}$ absorption at this wavelength was clearly observed.

Methyl viologen dication (MV^{2+}) is a well-known redox standard with E^0 = -0.44 V,[31] favored because of the very long lifetime and very strong absorption with λ_{max} at 605 nm of the reduced form $MV^{\bullet+}$. In the absence of impurities, the reduced $MV^{\bullet+}$ cation may be stable for weeks or longer. In the pulse radiolysis flow experiment this produces the requirement that the solution must be completely and thoroughly flushed between linac pulses so that signal averaging is not compromised by a buildup of the product. To avoid this problem, the results reported below are all from single-shot experiments in a sealed fused silica cuvette.

Fluorescein dye at pH > 7 is predominantly in the form of the dianion (F^{2-}) (the protonated monoanion FH^- pK_a = 6.4)[38] and is known to be reduced by e^-_{aq} forming semiquinone intermediates and λ_{max} ≈ 395 nm at pH 9 (semiquinone trianion S^{3-}).[39] The pK_a of the of the semiquinone dianion (SH^{2-}) is 9.5, as determined by flash photolysis.[40] Compton et al.[33] showed that one-electron reduction potential for fluorescein dianion (F^{2-}/S^{3-}) at pH 9.6 is -0.906 V *vs* SHE. The reduction potential of the protonated fluorescein monoanion (FH^-/SH^{2-}) at pH 6 measured by Compton et al.[34] was -0.724 V *vs* SHE.

$Ni(Me_6[14]4,11\text{-dieneN}_4)^{2+}$ (NMD^{2+}), and Ruthenium tris-bipyridyl ($Ru(bpy)_3^{2+}$) have the most negative reduction potentials, E^0 =-0.94 V *vs* SHE [35] and -1.3 V *vs* SHE [36] respectively, of the coordination compounds used in this study.

Table 1. Reference compounds used and their redox potentials, as well as the ion couples investigated with each compound.

Reference Compound	E^0 (V, SHE)	Ion Couple Investigated
$Ru(NH_3)_6^{3+/2+}$	0.05 [30]	$Co^{2+/+}$, $Ni^{2+/+}$, $Zn^{2+/+}$
$Co(en)_3^{3+/2+}$	-0.20 [8]	$Zn^{2+/+}$
$Cr(bpy)_3^{3+/2+}$	-0.26 [26]	$Co^{2+/+}$, $Ni^{2+/+}$, $Zn^{2+/+}$
$Co(sep)^{3+/2+}$	-0.30 [8]	$Co^{2+/+}$, $Ni^{2+/+}$
$MV^{2+/\bullet+}$	-0.44 [31,32]	$Co^{2+/+}$, $Ni^{2+/+}$
FH^{-}/SH^{2-}	-0.724 [33,34]	$Co^{2+/+}$, $Ni^{2+/+}$, $Zn^{2+/+}$
F^{2-}/S^{3-}	-0.906 [33,34]	$Co^{2+/+}$, $Ni^{2+/+}$, $Zn^{2+/+}$
$NMD^{2+/+}$	-0.94 [35]	$Co^{2+/+}$, $Ni^{2+/+}$, $Zn^{2+/+}$
$Ru(bpy)_3^{2+/+}$	-1.30 [36]	$Co^{2+/+}$, $Ni^{2+/+}$, $Zn^{2+/+}$

The monovalent ions, NMD^+ produced from the reactions with M^+ (2) or e^-_{aq} (3) were detected at 460 nm.[41] $Ru(bpy)_3^+$ was detected at 510 nm, representing a maximum difference of the $Ru(bpy)_3^+$ absorbance and $Ru(bpy)_3^{+2}$ bleach.[42]

The $^\bullet$OH radicals produced in irradiated aqueous systems were scavenged by either tertiary butyl alcohol (TBA)[43] or formate ion[1] (see Table 3).

3.1 Kinetics models of the radiation chemistry.

The kinetics models applied to extract the rate constants of the reactions of interest are mainly divided into two chemical systems based on the $^\bullet$OH radical scavenger employed: tert-butyl alcohol (TBA) or formate ion. In either case, we assume essentially a delta-pulse excitation (10ns or shorter) with the standard room temperature radiation chemistry yields:[44]

$$(H_2O)_{aq} \xrightarrow{\gamma} 2.73(e^-_{aq}) + 2.79(^\bullet OH)_{aq} + 0.6(^\bullet H)_{aq} + 0.45(H_2)_{aq} + 0.7(H_2O_2)_{aq} + 2.73(H^+)_{aq} \quad (7)$$

where the coefficients represent escape yields (G values) of the species in molecules/100eV. For fitting of the data, simulations are evaluated at 10ns/point by integration of the partial differential kinetic equations using a stiff equation solver with adaptive step size in the IGOR 6 software package of Wavemetrics.

3.1.1 TBA system. When TBA is added to the solutions, it will react with $^\bullet$OH radicals forming carbon-centered radicals (8). The rate constant at room temperature for this reaction is k_8 = 6×10^8 $M^{-1}s^{-1}$.[1]

$$(CH_3)_3COH + {}^\bullet OH \rightarrow H_2O + {}^\bullet CH_2(CH_3)_2COH \quad (8)$$

Likewise, TBA reacts with $^\bullet$H atom (9), but with a much lower rate constant,[43] $k_9 \approx 1\times10^5$ $M^{-1}s^{-1}$.

$$(CH_3)_3COH + {}^\bullet H \rightarrow H_2 + {}^\bullet CH_2(CH_3)_2COH \quad (9)$$

Since the $^\bullet$H atom reaction with TBA is relatively slow, the reactions of $^\bullet$H atom with the reduced forms of the metal ions (M^+) (10) and reduced reference compounds (A^{m-1}) (11) may be able to compete with reaction (9).

$M^+ + {}^\bullet H\ (+H^+) \rightarrow M^{2+} + H_2$ (10)
$A^{m-1} + {}^\bullet H\ (+H^+) \rightarrow A^m + H_2$ (11)

Moreover, the TBA radicals can undergo recombination reaction (12). Mezyk and Madden[45] have reported that the rate constant is k_{12} = 9.5×10^8 M^{-1}s^{-1}. The radical may also react with M^+ and A^{m-1} as shown in (13) and (14), respectively.

${}^\bullet CH_2(CH_3)_2COH + {}^\bullet CH_2(CH_3)_2COH \rightarrow$ products (12)
${}^\bullet CH_2(CH_3)_2COH + M^+ \rightarrow$ product (13)
${}^\bullet CH_2(CH_3)_2COH + A^{m-1} \rightarrow$ product (14)

The kinetics model for the systems with TBA is therefore composed of reactions (1) – (14).

3.1.2 Formate system. In a system with sodium formate, the formate ion will rapidly react with $^\bullet$OH (15) and $^\bullet$H atom (16) with rate constants k_{15} = 3.2×10^9 M^{-1}s^{-1} and k_{16} = 2.1×10^8 M^{-1}s^{-1}, that were taken from Buxton et al.[1]

$HCOO^- + {}^\bullet OH \rightarrow H_2O + CO_2^{\bullet-}$ (15)
$HCOO^- + {}^\bullet H \rightarrow H_2 + CO_2^{\bullet-}$ (16)

$CO_2^{\bullet-}$ radicals produced in reactions (15) and (16) can subsequently reduce the divalent metal ions (M^{2+}) (17) and the reference compounds (A^m) (18). The rate constants k_{17} and k_{18} in each system are summarized in Table 2.

$CO_2^{\bullet-} + M^{2+} \rightarrow CO_2 + M^+$ (17)
$CO_2^{\bullet-} + A^m \rightarrow CO_2 + A^{m-1}$ (18)

In addition, it is well-known that the $CO_2^{\bullet-}$ radicals can undergo self-recombination reaction (19) with a rate constant at room temperature, k_{19} = 5.0 × 10^8 M^{-1}s^{-1}.[11,46–48] In some cases, $CO_2^{\bullet-}$ can also react with the hyper-reduced metal ions (20)[15,19] and the reduced form of the reduced reference compounds (21).[36,39,41,42,49]

$CO_2^{\bullet-} + CO_2^{\bullet-} \rightarrow {}^-O_2CCO_2^-$ (19)
$CO_2^{\bullet-} + M^+\ (+H) \rightarrow$ products (20)
$CO_2^{\bullet-} + A^{m-1} \rightarrow$ product (21)

The kinetics models for the systems with formate in general contain reactions (1) – (6), (15) – (21). The rate constants for the e_{aq}^- reactions applied in the models are given in Table 2.

3.1.3 Ionic Strength The rate constants reported in this study have been corrected for ionic strength effect based on the Debye-Brønsted equation shown below.

$$\log(k_i) = \log(k_o) + 2AZ_1Z_2\sqrt{I} \quad \text{(E1)}$$

Here k_i and k_o are the rate constants at the ionic strength equal to i and *zero*, respectively, A is the Debye-Hückel constant calculated using Equation (E2), Z_1 and Z_2 are charges of reactants 1 and 2, respectively, I is the ionic strength (M).

Table 2. Rate constants of the e_{aq}^- and $CO_2^{\bullet-}$ reactions at zero ionic strength applied in the kinetics model (all in the unit of 10^7 M^{-1}s^{-1})

Reactant	Rate Constant (k×10^7 M^{-1}s^{-1})	
	e_{aq}^-	$CO_2^{\bullet-}$
Co^{2+}	1000 [3]	<0.01[19]
Zn^{2+}	160 [3]	0.002[15]
Ni^{2+}	2200[3]	<0.01 [19]
MV^{2+}	5000[49]	1000[49]
F^{2-}	1400 [39] (pH 10.8)	2.6 (pH 10.8) [39]
NMD^{2+}	4990[41]	2600 [41]
$Ru(bpy)_6^{2+}$	5800[42]	6[36]

$$A = \frac{e^3\{2N_A\}^{1/2}}{2.303\{8\pi\}\{\varepsilon_0 k_B T\}^{3/2}} \quad \text{(E2)}$$

Here N_A is the Avogadro's number, ε_0 is the vacuum permittivity and ε is the dielectric constant of the solvent.

3.2 Redox Kinetics of $Zn^{2+/+}$.

Unlike $Co^{2+/+}$ and $Ni^{2+/+}$ couples, we know an upper limit of E^0 for $Zn^{2+/+}$ (E^0 = -1.9 V) based on data obtained in experiments with Tl^+ by Ershov *et al*.[17,18] Thus, the possible redox potential range for the $Zn^{2+/+}$ couple is -1.9 V > E^0 > -2.87 V. In this study, we tested reference compounds with E^0 from 0.05 V to -1.3 V and $Zn^{2+/+}$ served as a standard, which should reduce all of these compounds. The rate constants obtained in this work are reported in Table 3.

3.2.1. The reaction of Zn^+ with $Co(en)_3^{3+}$ was investigated in TBA solutions (Fig. S1(A), supplementary information). The rate constant found for this reaction (Table 3) is four times smaller than the one published earlier (2×10^7 M^{-1}s^{-1} *vs* 9×10^7 M^{-1}s^{-1}, corrected to zero ionic strength).[50] This difference is attributed to the use of the sulfate counterion in reference [50], which likely ion pairs with the metal ion at the high concentrations (2×10^{-2} M) required for the measurement. In the reaction of Zn^+ with $Cr(bpy)_3^{3+}$ the growth of $Cr(bpy)_3^{2+}$ absorption was observed (Fig.S1(B)). The rate constant obtained is within error the same as previously reported (4.0×10^8 M^{-1}s^{-1} *vs* 5.4×10^8 M^{-1}s^{-1},[51] corrected to zero ionic strength).

Table 3. Rate constants (corrected to zero ionic strength) of the reactions studied (all in the unit of k×10^7 M^{-1}s^{-1}).

Reference Compound	Co^+	Ni^+	Zn^+	$^\bullet$OH scavenger
$Ru(NH_3)_6^{3+}$	2.9±0.1	0.4±0.1	81± 6	TBA
$Co(en)_3^{3+}$	-	-	2 ± 3	TBA
$Cr(bpy)_3^{3+}$	7.4±0.6	0.02±0.03	40 ±5	TBA
$Co(sep)^{3+}$	0.13±0.03	2.5 ±0.4	-	TBA
MV^{2+}	0.9±0.2	29 ± 2	-	Formate
F^{2-} / FH^-	<500 (pH 7.6)	<100 (pH 6.5)	<500 / 1660±800 (pH 6.5)	TBA/Formate
NMD^{2+}	x	x	20 ± 3	TBA/Formate
$Ru(bpy)_3^{2+}$	66 ± 6	x	55 ± 5	TBA/Formate

*x no reaction is observed; *- not studied

3.2.2. The reaction of Zn^+ with NMD^{2+} in formate solutions has been studied for the first time in this work. In the presence of NMD^{2+} (100-300 µM), Zn^+ was oxidized by the complex ion producing NMD^+ and Zn^{2+}. The results are illustrated in figure 1(A,B). Figure 1(A) shows the absorption signals *vs* wavelength as a 2-D waterfall plot obtained in reaction of Zn^+ with NMD^{2+}. In this experiment, most hydrated electrons react with Zn^{2+} giving Zn^+ ions that absorb at 310 nm. The fast decay of hydrated electrons is clearly seen at the longest wavelengths (550 nm). The reduced NMD^+ we detect from absorption peaks at 460 nm.

In figure 1(B) we isolate the initial kinetics of NMD^+ signals at 460 nm. In the blank solutions (without Zn^{2+}) hydrated electrons are promptly (within a microsecond) scavenged by NMD^{2+}. This is immediately followed by the reduction of NMD^{2+} by $CO_2^{\bullet-}$. The final signal amplitude is different for the two concentrations of NMD^{2+} because there is competition between NMD^{2+} scavenging and the self-recombination of $CO_2^{\bullet-}$. With addition of 50 mM Zn^{2+} ion, hydrated electrons are scavenged by Zn^{2+}, and the Zn^+ ions then quickly reduce NMD^{2+}. The Zn^+ reaction with NMD^{2+} does not produce quite the same concentration of NMD^+ because a fraction of Zn^+ is reduced by $CO_2^{\bullet-}$ giving Zn^0.

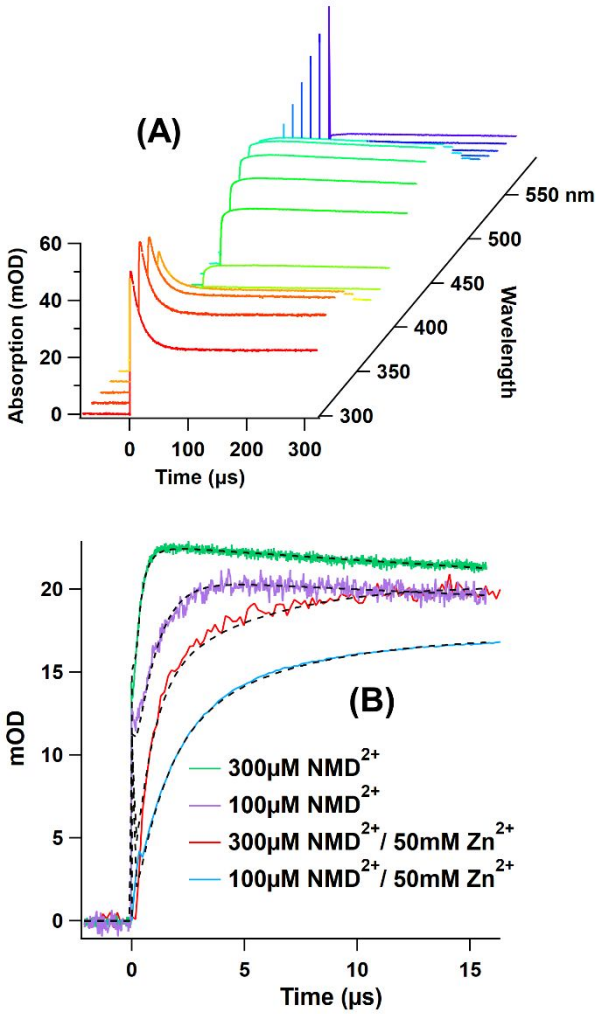

Fig. 1 (A) Transient absorption in the reaction of 300 µM NMD^{2+} with 5 mM Zn^{2+} in 10 mM formate solutions after 8 ns radiolysis pulse (~26 Gy); **(B)** NMD^+ signals at 460 nm in 10 mM formate solutions with 50 mM Zn^{2+}. The fit curves are shown in black.

The second order reaction between Zn^+ and $CO_2^{\bullet-}$ has been reported by Rabani and coworkers,[15] who claimed the rate constant for this reaction is 4×10^9 $M^{-1}s^{-1}$.

3.2.3. The fluorescein dye proves to be a useful reaction partner for the hyper-reduced metal ions of this study, with two accessible reduction potentials at E^o =-0.906 V for the dianion (F^{2-}) form, and -0.724 V for the (FH^-) protonated monoanion.[33,34] The corresponding reduced semiquinone species possess very strong absorption bands near 395 nm (S^{3-}) and 355 nm (SH^{2-}), respectively.[39,40,52] The pK_a for the fluorescein monoanion is 6.4,[38] so at this pH both F^{2-} and FH^- forms are equally available for reduction by the M^+ ions, or solvated electrons, or CO_2^- in formate solutions.

In figure 2(A) we plot the kinetics acquired at 393 nm and 357 nm following radiolysis of 100µM fluorescein with 0.1 M TBA at pH 6.5. Figure 2(B) illustrates the full spectra obtained in the 280—440 nm range at several delay times after the electron pulse. The hydrated electrons reduce F^{2-} to S^{3-} with rate constant of ca. 1.4×10^{10} $M^{-1}s^{-1}$, as reported in the literature,[39] giving very strong absorbance at 393 nm in the first 1—2 microseconds. Reduction of FH^- to SH^{2-} by hydrated electron also occurs on this timescale, with slightly smaller rate constant, giving strong absorbance at 357 nm. Within about 30 microseconds, all of the S^{3-} species has converted to the more stable SH^{2-} form, by some combination of proton transfer and electron transfer involving the F^{2-}/FH^- parent molecules:

$$S^{3-} + FH^- \leftrightarrow SH^{2-} + F^{2-} \qquad (22)$$

(The final product is reached several times more slowly in an experiment carried out at pH 7.5. Naturally, this equilibrium is also coupled to the acid-base equilibria of both the fluorescein dye and semiquinone ions.) The long-time decay visible in the kinetics at 357 nm is due to a recombination of SH^{2-} with the $^{\bullet}CH_2(CH_3)_2COH$ radicals.

Figure 2(C) illustrates the spectra acquired when 10 mM Zn^{2+} is added to the solution. Kinetics are also plotted in figure 2(A) for comparison with the blank. This Zn^{2+} concentration is sufficient to scavenge over 90 % of the hydrated electrons within 100ns. Unlike in the blank solution, we see no immediate reduction of F^{2-} to S^{3-}, followed by conversion of S^{3-} to SH^{2-}. Rather, we see direct reduction of the FH^- to SH^{2-} by the Zn^+ on nearly the same timescale:

$$Zn^+ + FH^- \rightarrow Zn^{2+} + SH^{2-} \qquad (23)$$

We estimate the rate constant for Zn^+ reduction of FH^- is 1.7×10^{10} $M^{-1}s^{-1}$. The rate constant for Zn^+ reduction of F^{2-} is at least five times slower, in spite of the larger driving force and greater coulomb attraction of the reactants.

The fluorescein system provides qualitatively very useful information, but it proved impossible to obtain a quantitative fit to the kinetics illustrated in Figure 2. Absorbance of the S^{3-} and SH^{2-} transients are superimposed on strong absorbances of the FH^- and F^{2-} parent ions. This is responsible for the pH-sensitive

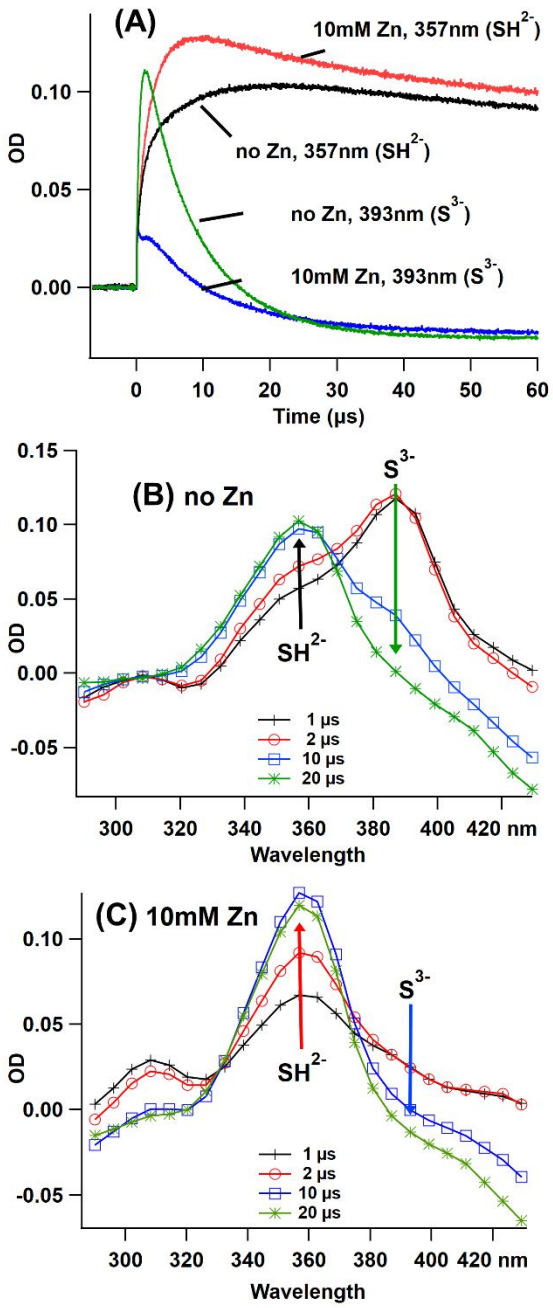

Fig. 2 Signals observed following 20 Gy radiolysis of pH 6.5 solutions of 100 μM fluorescein and 0.1 M TBA, with and without 10 mM added zinc perchlorate. **(A)** Kinetics at 357 and 393 nm. **(B)** Transient spectra observed without added Zn^{2+}. **(C)** Transient spectra in presence of 10 mM Zn^{2+}.

transient bleach apparent in the spectra of Figure 2. Moreover, the redox kinetics initiated by the hydrated electron is immediately coupled with kinetics of a pH-jump from simultaneous production of $(H^+)_{aq}$. The $^{\bullet}CH_2(CH_3)_2COH$ radicals produced from $^{\bullet}OH$ react with the semiquinone radicals with second order rate constant on the order of 3×10^8 $M^{-1}s^{-1}$ by either recombination or H atom abstraction, and without knowing the products it is difficult to predict their effect on the pH-jump.A similar problem arises from $^{\bullet}H$ atom reactions. Use of a 10 mM pH buffer would greatly simplify the kinetics, but would also remove any possibility to see growth of the S^{3-} transient. Finally, previous quantitative studies of the fluorescein dye kinetics have been carried out by flash photolysis,[40] where it is demonstrated that the long-lived triplet state of fluorescein ions will reduce or oxidize the ground state molecules. We expect that we excite this photochemistry as well with radiolysis, or even with the pulsed xenon analyzing lamp, to further complicate the situation.

3.2.4. The results obtained for Zn^{2+} with 40 μM $Ru(bpy)_3^{2+}$ (E^o = -1.3 V) in both formate and TBA containing solutions showed that Zn^+ reduces $Ru(bpy)_3^{2+}$ quantitatively, in agreement with the report of Meisel, et al.[42] The absorption signals following radiolysis of $Ru(bpy)_3^+$ are shown in figure 3(A) for the formate scavenger. Strong absorptions of $Ru(bpy)_3^+$ are superimposed on the bleach of the $Ru(bpy)_2^+$ parent ion at 450 nm. Maximum transient signal for $Ru(bpy)_3^+$ is found at 510 nm. At 300 nm, the Zn^+ absorbance is initially observed with limited S/N because probe light is severely attenuated by the parent $Ru(bpy)_3^{2+}$. Decay of the Zn^+ absorbance directly corresponds to additional growth at 510 nm.

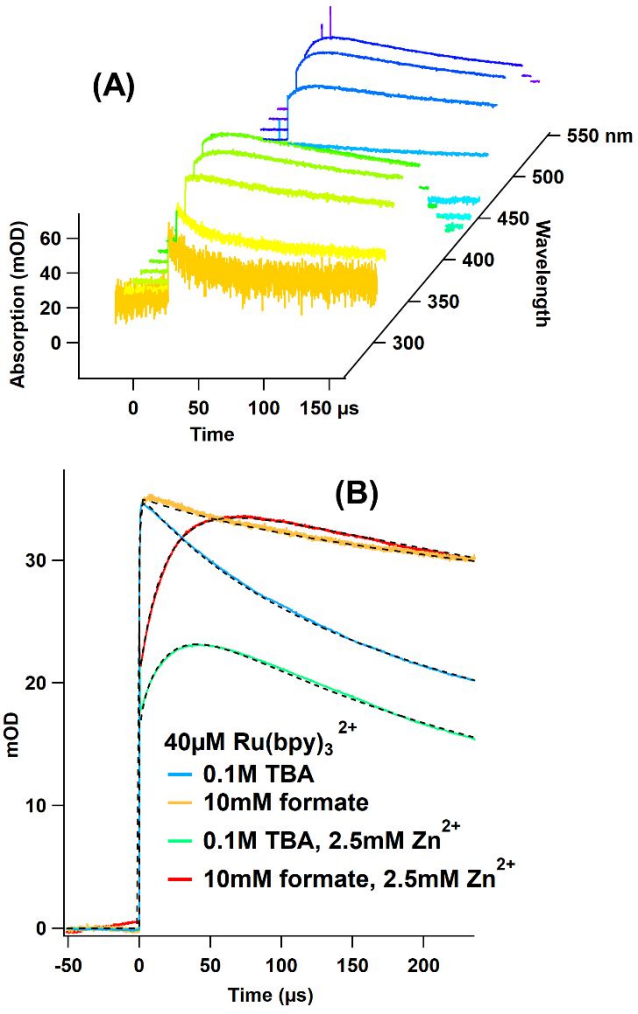

Fig. 3 (A) Transient absorption in the reaction of 40 μM $Ru(bpy)_3^{2+}$ with 2.5 mM Zn^{2+} in 10 mM formate solutions in 200 μs after 6ns pulse radiolysis (~23 Gy). **(B)** $Ru(bpy)_3^+$ decays at 510 nm in the mixtures of 40 μM $Ru(bpy)_3^{2+}$ and 2.5 mM Zn^{2+} in 0.1M TBA and in 10 mM formate solutions. The fit curves are shown in black.

The $Ru(bpy)_3^{+}$ signals at 510 nm are shown in figure 3(B) for both $^{\bullet}OH$ scavengers. In the blank solutions with only TBA, solvated electrons reduce the $Ru(bpy)_3^{2+}$ promptly. The subsequent decay over a millisecond timescale is due to second order recombination with the TBA radicals with a rate constant 1.2×10^9 $M^{-1}s^{-1}$ (14). Upon addition of 2.5 mM Zn^{2+}, part of the electrons reduce the added metal ion and the initial $Ru(bpy)_3^{+}$ transient at 510nm is attenuated. We can easily observe an additional signal growth in a 20—40 microsecond interval from the reduction by Zn^{+}. In the blank samples with formate, second order decay corresponding to the reaction between $Ru(bpy)_3^{+}$ and $CO_2^{\bullet-}$ radicals (21) occurs with a rate constant 6×10^7 $M^{-1}s^{-1}$.[36] An additional signal growth is detected up to 100 µs in the solutions with Zn^{2+}.

Thus, using Zn^{2+} solutions as an example, it has been shown that $Ru(NH3)_6^{3+}$, $Co(en)_3^{3+}$, $Cr(bpy)_3^{3+}$, NMD^{2+} , fluorescein, and $Ru(bpy)_3^{2+}$ can be used as reference compounds to study the redox potential of M^{+}.

3.3 Redox Kinetics of $Co^{2+/+}$.

3.3.1. The effects of $Ru(NH_3)_6^{3+}$ and $Co(sep)^{3+}$ on the decays of Co^{+} are shown in figure S2(A,B). TBA was used to scavenge the $^{\bullet}OH$ radical in this system. The influence of reference compounds ($Ru(NH_3)_6^{3+}$, $Co(sep)^{3+}$) on the decays of the Co^{+} signals was evident (Fig.S2(A) and Fig.S2(B)), suggesting that Co^{+} reduces these species by pseudo-first-order kinetics. In the case of $Cr(bpy)_3^{3+}$, the growth of the reduced form $Cr(bpy)_3^{2+}$ was observed at 560 nm (Fig.S2(C)). This set of experimental observations establish that E^0 for the $Co^{2+/+}$ couple must be more negative than -0.30 V which is the E^0 of $Co(sep)^{3+/2+}$.

3.3.2. Figure 4 shows the absorption of $MV^{\bullet+}$ at 600 nm on microsecond (A) and millisecond (B) timescales in 10 mM formate solutions and with/without a given concentration of Co^{2+}. In the blank solution, the initial growth of $MV^{\bullet+}$ absorption at 600 nm occurs within the first microsecond (Fig.4(A)). It is due to the reactions of MV^{2+} with the hydrated electron (3) and $CO_2^{\bullet-}$ (18) (from the formate scavenging of $^{\bullet}OH$ and $^{\bullet}H$ atoms). In solutions where Co^{2+} was present, the initial absorption of $MV^{\bullet+}$ at 600 nm was smaller. This is because a portion of the hydrated electron reacted with Co^{2+}, generating Co^{+} (1). At 100–200 µs period after the electron pulse, an additional growth of the absorbance was observed when the concentration of Co^{2+} was 10–30 mM. A plateau is reached by about 300 µs. The growing absorbance is evidence of the reaction of Co^{+} with MV^{2+}, producing $MV^{\bullet+}$ (2). It appears that there was no growth of $MV^{\bullet+}$ in the presence of Co^{2+} at a higher concentration (40 mM) and the $MV^{\bullet+}$ signal starts to decay away within 100 µs.

In figure 4(B) we follow the decay out to nearly 100 milliseconds with 100 µM solutions of MV^{2+} and various Co^{2+} concentrations. The $MV^{\bullet+}$ decay is dramatically sensitive to the concentration of Co^{2+}, with the half-life decreasing from on the order of one second at 10 mM Co^{2+}, to ca. 10 ms in the presence of 40 mM Co^{2+}.

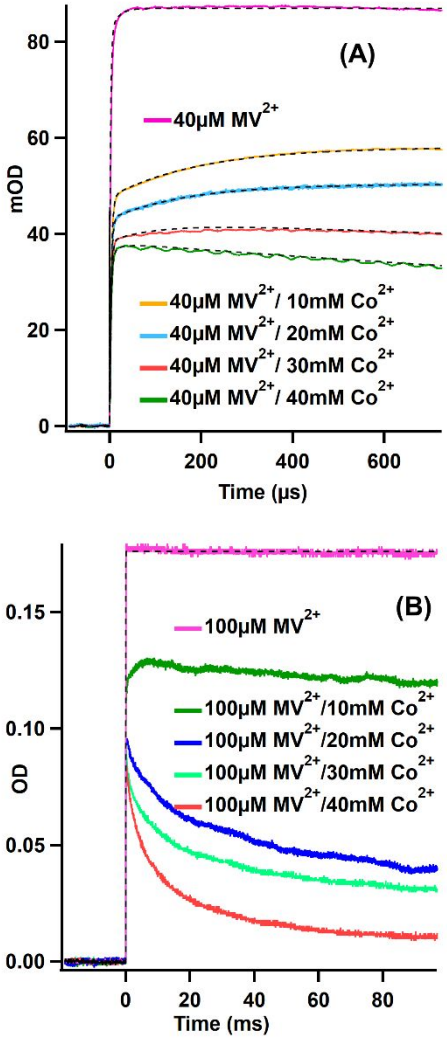

Fig. 4 $MV^{\bullet+}$ absorption at 600 nm in Co^{2+} solutions with 10 mM formate on microsecond **(A)** and millisecond **(B)** timescales. The fit curves are shown in black.

In a higher concentration range of the Co^{2+} systems (> 10 mM), the monovalent metal ions (Co^{+}) demonstrate a self-catalytic clustering behavior, as reported previously by Ershov and coworkers[53] in the gamma radiolysis of $Co^{2+}/MV^{\bullet+}$ solutions. Presumably the clusters become easier to reduce as they grow larger, explaining the extreme dependence of the $MV^{\bullet+}$ decay to the Co^{2+} concentration. The first step of this metal cluster formation must be that Co^{+} undergoes dimerization with Co^{2+} forming Co_2^{3+} (24).

$$Co^{+} + Co^{2+} \rightarrow Co_2^{3+} \qquad (24)$$

With this postulate, the growth and plateau kinetics of figure 4(A) can be interpreted as a competition for the Co^{+}, between reactions (2) and (24). The absorption signals do not follow the correct concentration dependence for an equilibrium between $MV^{\bullet+}$ and Co^{+}.

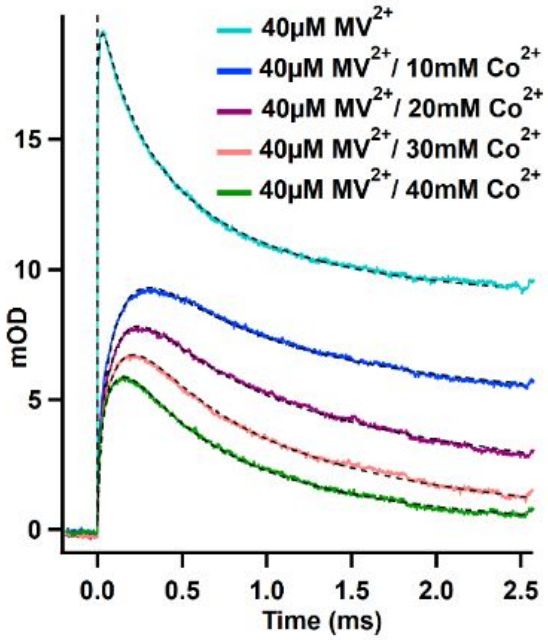

Fig. 5 $MV^{\bullet+}$ absorption at 600 nm in Co^{2+} solutions with 0.1 M TBA on millisecond timescale. The fit curves are shown in black.

Similar results were obtained when TBA was present in the solution, figure 5. The initial growth of $MV^{\bullet+}$ in the blank solution was caused by the reaction of MV^{2+} with e^-_{aq} (3), while a small secondary rise appearing in the first 100 μs is attributed to the reaction of $^{\bullet}H$ with MV^{2+} (11). The decay of $MV^{\bullet+}$ in this solution is due to the recombination reaction with the TBA radical (14). In the solutions with Co^{2+}, most of the hydrated electrons are scavenged by the divalent metal ion thus generating Co^{+} (1). Therefore, $MV^{\bullet+}$ detected under these conditions is overwhelmingly produced by the reduction of MV^{2+} by Co^{+} (2). The absorbance growth from the reaction with $^{\bullet}H$ (11) shows that it contributes minor concentrations of product. The reaction of $MV^{\bullet+}$ with the TBA radical in combination with the oxidation by the self-catalysis product, Co_2^{3+} (24), is responsible for the decays of $MV^{\bullet+}$ in the Co^{2+} containing solutions at longer times.

A rate constant, 5.2×10^4 $M^{-1}s^{-1}$, for the dimerization was obtained from the model. Based on the reduction of MV^{2+} by Co^{+} an upper limit for the E^0 of $Co^{2+/+}$ is shifted to -0.44 V.

3.3.3. The reaction of Co^{+} with NMD^{2+} in formate solutions has been studied for the first time in this work. In the solutions containing 150 μM NMD^{2+} and 10mM formate no reaction of Co^{+} with NMD^{2+} was observed (Fig.S3), or reaction of Co^{2+} with NMD^{+}.

3.3.4. Prompt reactions of Co^{+} ion with fluorescein ions F^{2-} and FH^{-} are illustrated by the transient spectra in Figure 6. A pH 7.6 solution of 10 mM Co^{2+} containing 0.1 M TBA and 50 μM fluorescein was irradiated with a 18Gy electron pulse. At this Co^{2+} concentration, hydrated electrons are converted to Co^{+} within about 10 ns. Signals from both the S^{3-} and SH^{2-} semiquinone species grow in the first two microseconds, with ratio of approximately 2:1.

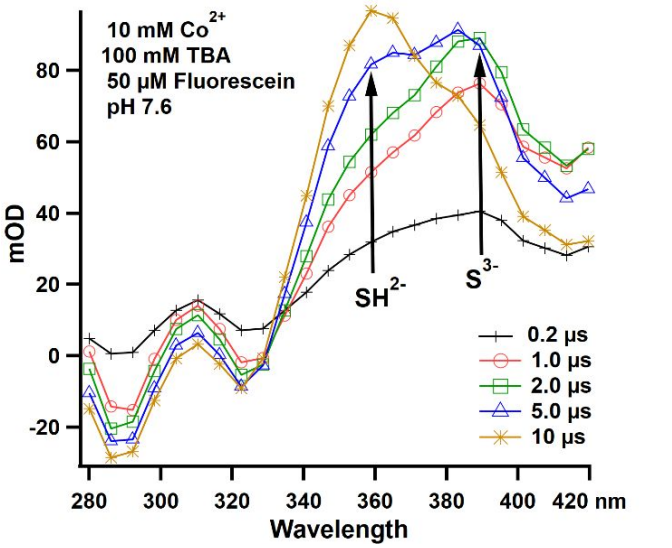

Fig. 6 Transient spectra in 10 mM Co^{2+} / 50 μM fluorescein / 0.1 M TBA solutions at pH 7.6. Prompt growth of both semiquinone trianion S^{3-} and protonated dianion SH^{2-} are observed.

The S^{3-} signal mostly converts to SH^{2-} within roughly 30 microseconds, in competition with the recombination with $^{\bullet}CH_2(CH_3)_2COH$ radicals. The pK_a of FH^{-} is 6.4, so at pH 7.6, the ratio of F^{2-}/FH^{-} is 16:1. We infer that the ratio of rate constants is roughly 8:1 in favor of the Co^{+} reduction of FH^{-} over F^{2-}, a result similar to that found for Zn^{+} in section 3.2.3. The Co^{+} apparently also reduces impurity added with the TBA, so the absolute rate constants are not available.

The observation of Co^{+} reduction of F^{2-} ion proves $E_0 < -0.906$ V for the $Co^{2+/+}$ couple.

3.3.5. The reactions of 40 μM $Ru(bpy)_3^{2+}$ with Co^{+} have been studied in both TBA and formate solutions (Fig.7). Meisel, et al.[42] reported a quick survey of the other first-row transition metal ions beyond Zn^{2+}, and concluded that none of the other M^{+} species would reduce $Ru(bpy)_3^{2+}$ except for cobalt. The report of Meisel, et al.[42] is confusing because they claimed the absorbance signals in presence of Co^{2+} were similar to those of Zn^{2+}. We find them significantly different (c.f. figure 3(B)).

In TBA and formate solutions with 40 μM $Ru(bpy)_3^{2+}$ and 2.5 mM Co^{2+}, the initial $Ru(bpy)_3^{+}$ transient at 510 nm is greatly attenuated relative to the blank solution (Figure 7). The signal amplitudes reach roughly half of their values in the blank experiment. Within the S/N of the illustrated experiment we can conclude that Co^{+} does reduce $Ru(bpy)_3^{2+}$ producing additional signal growth by 20—40 μs. The full spectrum was recorded in each case and the signal growth does seem to be from production of $Ru(bpy)_3^{+}$ rather than some other product.

Unlike results obtained with $Ru(bpy)_3^{2+}$ and Zn^{+}, we see the contribution of secondary reactions to the $Ru(bpy)_3^{+}$ signal decay. To fit the curves, we included the formation of cobalt clusters in the kinetics (24). To explore this more thoroughly we carried out experiments with different concentrations of cobalt and formate (Fig. S4(A,B)). With an increase in the concentration of cobalt (Fig. S4(B)), the second order decay of the signal appears to be faster because product clusters Co_2^{3+} oxidize (react with) $Ru(bpy)_3^{+}$ with a rate constant 9×10^8 $M^{-1}s^{-1}$.

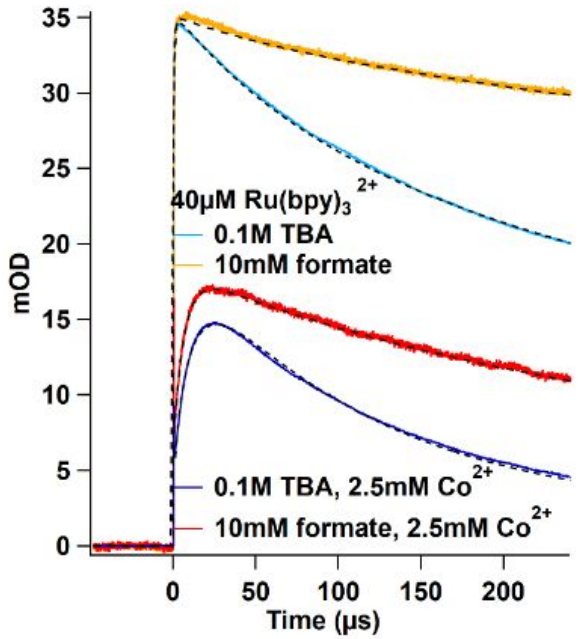

Fig. 7 $Ru(bpy)_3^+$ decays at 510 nm in the mixtures of 40 μM $Ru(bpy)_3^{2+}$ and 2.5 mM Co^{2+} in 0.1 M TBA (blue)and in 10 mM formate (red) solutions. The fit curves are shown in black.

As can be seen from figure S4(A), different concentrations of formate affect the kinetics by way of ionic strength effect on the reaction rates, which we took into account when fitting the data. These results suggest that Co^+ reduces $Ru(bpy)_3^{2+}$ with a rate constant 6.6×10^8 $M^{-1}s^{-1}$.

The demonstrated reaction of $Ru(bpy)_3^{2+}$ with Co^+ provides the most positive rigorous upper limit of $E^o < -1.3$ V for the $Co^{2+/+}$ couple that we are able to find.

3.4 Redox Kinetics of $Ni^{2+/+}$.

3.4.1. The reactions of Ni^+ with $Ru(NH_3)_6^{3+}$, $Co(sep)^{3+}$ and $Cr(bpy)_3^{2+}$ were investigated with the aim to learn about the $Ni^{2+/+}$ redox potentials. Fits of the traces obtained from these reactions suggest that Ni^+ can reduce all three compounds (Figures S5(A-C)). Therefore E^0 of the $Ni^{2+/+}$ couple is less than -0.30 V.

3.4.2. In the reaction of Ni^+ with MV^{2+} in formate solutions the transient absorption recorded at 600 nm indicates that all of the Ni^+ ions produced were converted into $MV^{\bullet+}$ via reaction (2), with the rate constant 2.9×10^8 $M^{-1}s^{-1}$ (Fig.S5(D)). These results move the positive limit for the E^0 of $Ni^{2+/+}$ to -0.44 V.

3.4.3. Ni^+ reactions with fluorescein anions were investigated at pH 6.5 with both TBA and formate OH scavengers. The experiment with 10 mM Ni^{2+}, 10 mM formate, and 100 μM fluorescein at pH 6.5 is shown as a 2-D waterfall plot in figure 8(A). In addition to the expected semiquinone bands of SH^{2-} and S^{3-} at 355 nm and 395 nm respectively, we found an additional strong band at 310 nm from the Ni^{2+} absorbance and a large transient at 420 nm from bleach/pH-jump of FH^-/F^{2-}. Figure 8(B) shows the development of spectra across the 280—420 nm range at several representative delay times (after the electron pulse), pointing out the dominant absorption bands. Figure 8(C) shows kinetic traces corresponding to the absorbance maxima of the four bands, over the first 20 μs. Figure 8(D) shows the same wavelengths out to 150 μs. A similar experiment with 0.1 M TBA scavenger is illustrated in Figure S6.

The earliest spectrum of figure 8(B) at 100 ns after the pulse shows only a band around 310 nm. This is the absorbance due to Ni^+ itself. At 10 mM concentration of Ni^{2+}, the hydrated electron scavenging reaction will be over within roughly the 20 ns time step of the trace. The signal appears as a time-zero step in the 304 nm trace of figure 8(C). The absorbance at 304 nm changes little in the first several microseconds, but absorbance of the other three bands grow in (Fig.8(C)), with similar time constants. This first stage of signal growth appears to be over at approximately 5 μs. The absorbance at 420 nm is completely dominated by the fluorescein monoanion, so we ascribe this initial growth to capture of radiolytic protons by F^{2-}.

The initial absorbance growth at 355 and 395 nm is a combination of bleach/pH-jump of the fluorescein anions and reduction of FH^- and F^{2-} by Ni^+ giving the SH^{2-} and S^{3-}, respectively. At about 5 μs, the bleach/pH-jump kinetics at 420 nm diverge from the S^{3-} and SH^{2-} kinetics. The 420 nm signal is dominated at longer time by depletion of FH^- as the protons equilibrate among the several products.

The Ni^+ absorbance at 304 nm has lifetime of roughly 20 μs, and this decay is probably dominated by Ni^+ reduction of the fluorescein anions. We can see that the maximum absorbance of S^{3-} at 395 nm occurs at about 8 μs. At longer time, once Ni^+ is depleted, the electron/proton exchange reaction (22) converts all S^{3-} to SH^{2-} absorption at 355 nm.

At very long time, past 50 μs, the FH^- bleach at 420 nm continues to increase along with the SH^{2-} absorption at 355 nm. This is certainly due to relatively slow reduction reactions by the $CO_2^{\bullet-}$ radical from formate. However, the bleach increases faster than we can account for from reduction of FH^- alone. We postulate that there is simultaneously a reduction reaction of the SH^{2-} ion to the leuco-dye, which consumes two protons (or two FH^-) and decreases the SH^{2-} absorption.

Clearly, Ni^+ can reduce fluorescein ions to the more stable SH^{2-} product. For the purpose of the present study, the important thing is the demonstration, in figures 8(B) and 8(C), that Ni^+ ion can directly reduce the F^{2-} ion to S^{3-} (S6(B) and S6(C) for the TBA scavenger). This proves that $E^0 < -0.906$ V for the $Ni^{2+/+}$ couple.

3.4.4. In the experiments of Ni^+ (2.5 mM Ni^{2+}) with 150 μM NMD^{2+} we saw no reactions, so no conclusions can be drawn (Fig.S3).

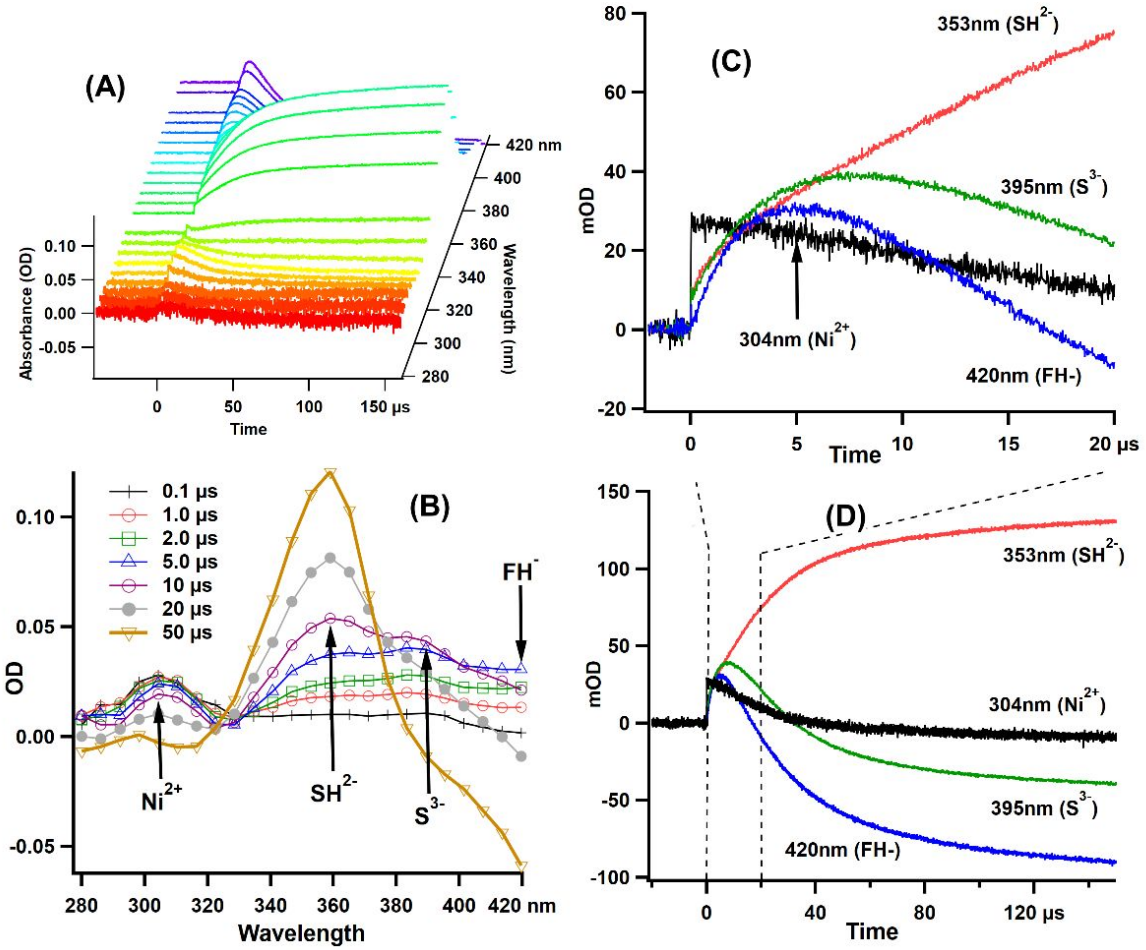

Fig. 8 (A) Transient absorption in 100 µM fluorescein solutions with 10 mM Ni^{2+} and 10 mM formate at pH 6.5. **(B)** Spectra extracted from (A) at several points in the kinetic development. The four major transients are indicated. **(C)** Kinetics traces showing signal growth at four wavelengths corresponding to the four major transients. **(D)** Development of the signals in (C) out to 150 µs.

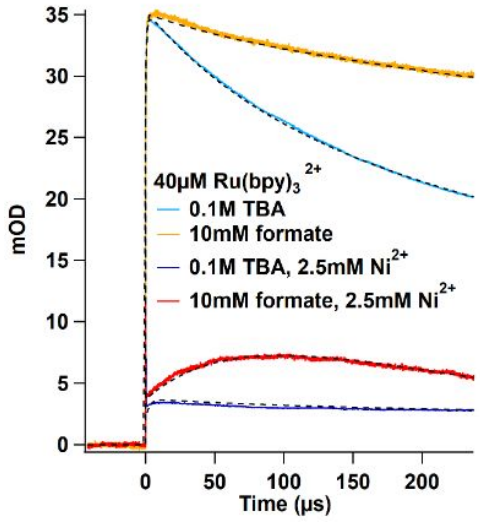

Fig.9 $Ru(bpy)_3^+$ decays at 510 nm in the mixtures of 40 µM $Ru(bpy)_3^{2+}$ and 2.5 mM Ni^{2+} in 0.1 M TBA (red) and in 10 mM formate (blue) solutions. The fit curves are shown in black.

3.4.5. We performed experiments of Ni^{2+} with 40 µM $Ru(bpy)_3^{2+}$ with both •OH radical scavengers, TBA and formate. Figure 9 illustrates the kinetics observed upon radiolysis of $Ru(bpy)_3^{2+}$ solutions. In the presence of 2.5 mM Ni^{2+}, initial absorption signal of $Ru(bpy)_3^+$ is decreased. In the TBA solutions there was no evidence that Ni^+ can reduce $Ru(bpy)_3^{2+}$. In the case of formate solutions (Fig. 9) a signal growth was observed after 50 µs in the presence of Ni^{2+}. In this case, the signal growth rate is 6×10^7 $M^{-1}s^{-1}$, which corresponds to the rate of formation of $Ru(bpy)_3^+$ from reaction with $CO_2^{\bullet-}$.[42] The same growth occurs in the "blank" solution, but is masked by the simultaneous second order recombination. Therefore, based on the data obtained in the experiment of Ni^{2+} with 40 µM $Ru(bpy)_3^{2+}$, we do not find any reaction, in agreement with the assertion of Meisel, et al.[42]

Accordingly, the redox potential values for the nickel couple $Ni^{2+/+}$ remains in the range, -1.9 V< E^0 < -0.906 V *vs* SHE.

Conclusions

This work has focused on minimizing the very large uncertainty in the reduction potentials of aqueous ion pairs $Co^{2+/+}$ and $Ni^{2+/+}$, by measuring the reactions of the metal species with various reaction partners having known reduction potentials. For the Co^{2+} system, we have confirmed upper and lower limits already present in the literature;[2,42] the E^o must lie between that of CO_2^- at -1.90 V, and that of $Ru(bpy)_3^{2+}$ at -1.3 V *vs* SHE. For the Ni^{2+} system, we have substantially reduced the uncertainty range of E^o by measuring the reaction of Ni^+ with fluorescein dianion F^{2-}; the E^o must lie between that of CO_2^- at -1.90 V, and that of F^{2-} at -0.906 V.[2,33] The Ni^+ ion does not readily reduce the $Ru(bpy)_3^{2+}$, suggesting E^o for the $Ni^{2+/+}$ couple may be less negative than -1.3 V. Failure to see this reaction proves nothing, but it does agree with the *ab initio* predictions of Rempe and coworkers,[25] who calculate E^o = -1.0 or -1.3 V depending on method.

Measurement of the reduction reactions for $Co^{2+/+}$ was greatly complicated by the clustering reactions of the reduced Co^+ with its parent hexa-aquo dication. The self-catalyzed clustering was already demonstrated in the gamma-irradiated methyl viologen system by Ershov, et al.[53] In this work we determined for the first time the rate constants for the initial dimerization and trimerization steps. This was needed to confirm the earlier claim of Meisel et al.[42] in the $Ru(bpy)_3^{2+}$ system.

Rate constants for the reduction of a number of redox standards by M^+ (M = Zn, Co, Ni) are compiled in Table 3. It has become obvious to us that aromatic compounds are the most likely to be reduced by M^+. The reduction of Ni^{2+} by $CO_2^{\bullet-}$ radical is quite slow in spite of the large driving force, and reduction of Ni^{2+} or Co^{2+} by $^\bullet H$ atoms are not even observed in spite of the even larger driving force (for $^\bullet H/H^+$ E^0= -2.3 V).[54] The reduction of Ni^{2+} by Zn^+ cannot be measured.[2] In terms of the Marcus electron transfer theory,[21,22] these observations are consistent with both a large reorganization energy, and generally poor overlap of the initial and final wave functions (the aromatic compounds provide the best overlap). The aqueous M^{2+} ions are known to be coordinated by six water molecules. Infrared spectroscopic studies of M^+ clusters in the gas phase have found that fewer than six water molecules are directly bound to the metal.[55–57] For Zn^+, the first three waters bind directly to the metal.[56] Additional water molecules form hydrogen bonds to these four, based on the OH stretching frequencies. In the case of Ni^+, only four water molecules are bound to metal,[57] and for Co^{2+} three water molecules are coordinated.[55] The implication is that for electron transfer reactions of the $M^{2+/+}$ ions, several water molecules must be lost or added, and this large reorganization of the solvation shell must dramatically reduce the reaction probabilities. It explains why the reduction potentials of these transition metal pairs have been so difficult to determine.

Conflicts of interest

There are no conflicts to declare.

Acknowledgements

The authors would like to thank Dr. Guillermo Ferraudi and Dr. Daniel M. Chipman for a number of helpful discussions.
This work is supported by the U.S. Department of Energy, Office of Science, Office of Basic Energy Sciences under award number DE-FC02-04ER15533. This is document number NDRL-5289 from the Notre Dame Radiation Laboratory.

1 G. V. Buxton, C. L. Greenstock, W. P. Helman and A. B. Ross, Critical Review of rate constants for reactions of hydrated electrons, hydrogen atoms and hydroxyl radicals ($^\cdot OH/^\cdot O^-$ in Aqueous Solution, *J. Phys. Chem. Ref. Data*, 1988, **17**, 513–886.

2 G. V. Buxton and R. M. Sellers, The radiation chemistry of metal ions in aqueous solution, *Coord. Chem. Rev.*, 1977, **22**, 195–274.

3 K. Kanjana, B. Courtin, A. MacConnell and D. M. Bartels, Reactions of Hexa-aquo Transition Metal Ions with the Hydrated Electron up to 300 °C, *J. Phys. Chem. A*, 2015, **119**, 11094–11104.

4 C. C. Lin, A review of corrosion product transport and radiation field buildup in boiling water reactors, *Prog. Nucl. Energy*, 2009, **51**, 207–224.

5 K. I. Choudhry, D. T. Kallikragas and I. M. Svishchev, On the thermochemical hydrogen release rate and activity transport in a supercritical water-cooled reactor, *Mater. Corros.*, 2016, **67**, 804–809.

6 A. J. Bard, R. Parsons and J. Jordan, *Standard Potentials in Aqueous Solution*, Routledge, 2017.

7 S. G. Bratsch, Standard Electrode Potentials and Temperature Coefficients in Water at 298.15 K, *J. Phys. Chem. Ref. Data*, 1989, **18**, 1–21.

8 J. F. Endicott, K. Kumar, T. Ramasami and F. P. Rotzinger, in *Progress in Inorganic Chemistry: An Appreciation of Henry Taube*, John Wiley and Sons Inc., 2007, vol. 30, pp. 141–187.

9 H. Strehlow, in *Berichte der Bunsengesellschaft für physikalische Chemie*, 1978, vol. 82, pp. 1114–1114.

10 D. D. M. Wayner, D. J. McPhee and D. Griller, Oxidation and Reduction Potentials of Transient Free Radicals, *J. Am. Chem. Soc.*, 1988, **110**, 132–137.

11 J. P. Baxendale, J. H.; Fielden, E. M.; Keene, The pulse radiolysis of aqueous solutions of some inorganic compounds, *Proc. R. Soc. London. Ser. A. Math. Phys. Sci.*, 1965, **286**, 320–336.

12 J. H. Baxendale and R. S. Dixon, Some unusual reductions by the hydrated electron, *Proc. Chem. Soc.*, 1963, 148–149.

13 N. Basco, S. K. Vidyarthi and D. C. Walker, Hydrated Electrons Produced by the Flash Photolysis of Co^+, Ni^+, Zn^+, and Cd^+ Ions, *Can. J. Chem.*, 1974, **52**, 343–347.

14 U. Schmidhammer, P. Pernot, V. De Waele, P. Jeunesse, A. Demarque, S. Murata and M. Mostafavi, Distance Dependence of the Reaction Rate for the Reduction of Metal Cations by Solvated Electrons: A Picosecond Pulse Radiolysis Study, *J. Phys. Chem. A*, 2010, **114**, 12042–12051.

15 J. Rabani, W. A. Mulac and M. S. Matheson, Pulse radiolysis studies of Zn^+ reactions, *J. Phys. Chem.*, 1977, **81**, 99–104.

16 M. Domae, N. Chitose, Z. Zuo and Y. Katsumura, Pulse radiolysis study on redox reactions of zinc(II), *Radiat. Phys.*

Chem., 1999, **56**, 315–322.

17 B. G. Ershov, E. Janata and A. Henglein, Mixed Metal Clusters in Aqueous Solution: Reactions of Cd^+, Co^+, Zn^+, and Ni^+ with Ag^+, *J. Phys. Chem.*, 1994, **98**, 7619–7623.

18 B. G. Ershov, E. Janata and A. Henglein, Mixed-Metal Clusters in Aqueous Solution: Reactions of Tl^{2+} with Ag^+, Cd^{2+}, and Pb^{2+} and of Zn^+ with Tl^+, *J. Phys. Chem.*, 1994, **98**, 10891–10894.

19 G. V. Buxton and R. M. Sellers, Pulse radiolysis study of monovalent cadmium, cobalt, nickel and zinc in aqueous solution. Part 1. - Formation and decay of the monovalent ions, *J. Chem. Soc. Faraday Trans. 1 Phys. Chem. Condens. Phases*, 1975, **71**, 558–567.

20 J. H. Baxendale and R. S. Dixon, Reactions of the Reducing Species in the Radiolysis of Aqueous Methanol Solutions, *Zeitschrift fur Phys. Chemie*, 1964, **43**, 161–176.

21 A. Nitzan, Chemical Dynamics in Condensed Phases. Relaxation, Transfer and Reactions in Condensed Matter Molecular Systems. By Abraham Nitzan., *ChemPhysChem*, 2007, **8**, 1250–1252.

22 S. Fletcher, The theory of electron transfer, *J. Solid State Electrochem.*, 2010, **14**, 705–739.

23 G. Navon and D. Meyerstein, The reduction of ruthenium (III) hexaammine by hydrogen atoms and monovalent zinc, cadmium, and nickel ions in aqueous solutions, *J. Phys. Chem.*, 1970, **74**, 4067–4070.

24 G. V. Buxton, F. Dainton and D. R. McCracken, Radiation chemical study of the reaction of Ni^+, Co^+ and Cd^+ with N_2O. Evidence for the formation of a hyperoxidised state by oxygen atom transfer, *J. Chem. Soc. Faraday Trans. 1 Phys. Chem. Condens. Phases*, 1973, **69**, 243–254.

25 D. Jiao, K. Leung, S. B. Rempe and T. M. Nenoff, First Principles Calculations of Atomic Nickel Redox Potentials and Dimerization Free Energies: A Study of Metal Nanoparticle Growth, *J. Chem. Theory Comput.*, 2011, **7**, 485–495.

26 B. R. Baker and B. D. Mehta, Polarography and Oxidation-Reduction Reactions of the Chromium(II) and Chromium (III) Complexes of 2,2'-Bipyridine, *Inorg. Chem.*, 1965, **4**, 848–854.

27 S. M. Nelson, Developments in the synthesis and coordination chemistry of macrocyclic Schiff base ligands, *Pure Appl. Chem.*, 2007, **52**, 2461–2476.

28 N. F. Curtis, Y. M. Curtis and H. K. J. Powell, Transition-metal complexes with aliphatic Schiff bases. Part VIII. Isomeric hexamethyl-1,4,8,11-tetra-azacyclotetradecadienenickel(II) complexes formed by reaction of trisdiaminoethanenickel(II) with acetone, *J. Chem. Soc. A Inorganic, Phys. Theor.*, 1966, 1015.

29 G. V. Buxton and C. R. Stuart, Re-evaluation of the thiocyanate dosimeter for pulse radiolysis, *J. Chem. Soc. Faraday Trans.*, 1995, **91**, 279.

30 E. L. Yee, R. J. Cave, K. L. Guyer, P. D. Tyma and M. J. Weaver, A Survey of Ligand Effects upon the Reaction Entropies of Some Transition Metal Redox Couples, *J. Am. Chem. Soc.*, 1979, **101**, 1131–1137.

31 D. M. Stanbury, Reduction Potentials Involving Inorganic Free Radicals in Aqueous Solution, *Adv. Inorg. Chem.*, 1989, **33**, 69–138.

32 P. S. Rao and E. Hayon, Redox Potentials of Free Radicals. I. Simple Organic Radicals, *J. Am. Chem. Soc.*, 1974, **96**, 1287–1294.

33 R. G. Compton, R. G. Harland, P. R. Unwin and A. M. Waller, Rotating-disc electrodes. ECE and DISP1 processes, *J. Chem. Soc. Faraday Trans. 1 Phys. Chem. Condens. Phases*, 1987, **83**, 1261.

34 R. G. Compton, D. Mason and P. R. Unwin, The reduction of fluorescein in aqueous solution (at pH 6). A new DISP2 reaction, *J. Chem. Soc. Faraday Trans. 1 Phys. Chem. Condens. Phases*, 1988, **84**, 483–489.

35 J. F. Endicott, D. P. Rillema and E. Papaconstantinou, Oxidation-reduction behavior of complexes containing macrocyclic ligands. Electrochemical comparison of complexes with the metals iron through zinc, *Inorg. Chem.*, 1971, **10**, 1739–1746.

36 M. D'Angelantonio, Q. G. Mulazzani, M. Venturi, M. Ciano and M. Z. Hoffman, One-electron reduction of ruthenium(II)-diimine complexes. Characterization of reduced species containing 2,2'-bipyridine, 2,2'-bipyrimidine, and 2,2'-bipyrazine in aqueous solution, *J. Phys. Chem.*, 1991, **95**, 5121–5129.

37 G. J. Ferraudi and J. F. Endicott, Excited state redox chemistry of polypyridyl chromium(III) complexes. A determination of the chromium(III)–(II) self-exchange rate [1], *Inorganica Chim. Acta*, 1979, **37**, 219–223.

38 R. Sjöback, J. Nygren and M. Kubista, Absorption and fluorescence properties of fluorescein, *Spectrochim. Acta Part A Mol. Biomol. Spectrosc.*, 1995, **51**, L7–L21.

39 P. Cordier and L. I. Grossweiner, Pulse radiolysis of aqueous fluorescein, *J. Phys. Chem.*, 1968, **72**, 2018–2026.

40 L. Lindqvist, in *Arkiv for Kemi*, Almqvist & Wiksell, 1960, vol. 16(8), p. 79.

41 A. M. Tait, M. Z. Hoffman and E. Hayon, Reactivity of Nickel(I) and Copper(I) Complexes Containing 14-Membered Macrocyclic Ligands in Aqueous Solution, *Inorg. Chem.*, 1976, **15**, 934–939.

42 D. Meisel, M. S. Matheson, W. A. Mulac and J. Rabani, Transients in the flash photolysis of aqueous solutions of tris(2,2'-bipyridine)ruthenium(II) ion, *J. Phys. Chem.*, 1977, **81**, 1449–1455.

43 S. V. Lymar and H. A. Schwarz, Hydrogen atom reactivity toward aqueous tert-Butyl alcohol, *J. Phys. Chem. A*, 2012, **116**, 1383–1389.

44 A. J. Elliot and D. M. Bartels, The Reaction Set, Rate Constants and g-Values for the Simulation of the Radiolysis of Light Water Over the Range 20 to 350 C Based on Information Available in 2008, *At. Energy Canada Ltd. Rep.*, 2009, 153–127160.

45 S. P. Mezyk and K. P. Madden, Self-Recombination Rate Constants for 2-Propanol and tert-Butyl alcohol Radicals in Water, *J. Phys. Chem. A*, 1999, **103**, 235–242.

46 M. A. Thomas, C. Capeillere-Blandin, J. Pucheault and C. Ferradini, Pulse radiolysis study of a yeast cytochrome c from Hansenula anomala, *Biochimie*, 1986, **68**, 745–755.

47 C. Capeillere-Blandin, J. Pucheault and C. Ferradini, The reduction of flavocytochrome b2 by carboxylate radicals. A pulse radiolysis study, *Biochim. Biophys. Acta (BBA)/Protein Struct. Mol.*, 1984, **786**, 67–78.

48 J. P. Keene, Y. Raef and A. J. Swallow, in *Pulse Radiolysis*, eds.

M. Emert, J. P. Keene and A. J. Swallow, Academic Press, London, New York, 1965, pp. 99–106.

49 N. Chitose, Y. Katsumura, M. Domae, Z. Cai, Y. Muroya, T. Murakami and J. A. LaVerne, Radiolysis of Aqueous Solutions with Pulsed Ion Beams. 4. Product Yields for Proton Beams in Solutions of Thiocyanate and Methyl Viologen/Formate, *J. Phys. Chem. A*, 2001, **105**, 4902–4907.

50 D. Meyerstein and W. A. Mulac, Reduction of cobalt(III) complexes by monovalent zinc, cadmium, and nickel ions in aqueous solutions, *J. Phys. Chem.*, 1969, **73**, 1091–1095.

51 G. A. Lawrance and D. F. Sangster, Reactions of chromium(III) complexes of 1,10-phenanthroline, 2,2′-bipyridyl, and oxalate with the pulse radiolytically generated aquated electron, zinc(I), and cadmium(I), *J. Chem. Soc. Dalt. Trans.*, 1987, 1425–1429.

52 U. Krüger and R. Memming, Formation and Reactions of Long Lived Xanthene Dye Radicals. II. Photochemical Reduction of Rhodamine-B and Fluoresceïn Derivatives, *Berichte der Bunsengesellschaft für Phys. Chemie*, 1974, **78**, 679–685.

53 B. G. Ershov, N. L. Sukhov and E. Janata, Formation, absorption spectrum, and chemical reactions of nanosized colloidal cobalt in aqueous solution, *J. Phys. Chem. B*, 2000, **104**, 6138–6142.

54 D. A. Armstrong, R. E. Huie, W. H. Koppenol, S. V. Lymar, G. Merenyi, P. Neta, B. Ruscic, D. M. Stanbury, S. Steenken and P. Wardman, Standard electrode potentials involving radicals in aqueous solution: Inorganic radicals (IUPAC Technical Report), *Pure Appl. Chem.*, 2015, **87**, 1139–1150.

55 K. Furukawa, K. Ohashi, N. Koga, T. Imamura, K. Judai, N. Nishi and H. Sekiya, Coordinatively unsaturated cobalt ion in $Co^{+}(H_2O)_n$ (n = 4-6) probed with infrared photodissociation spectroscopy, *Chem. Phys. Lett.*, 2011, **508**, 202–206.

56 B. Bandyopadhyay, K. N. Reishus and M. A. Duncan, Infrared Spectroscopy of Solvation in Small $Zn^{+}(H_2O)_n$ Complexes, *J. Phys. Chem. A*, 2013, **117**, 7794–7803.

57 R. S. Walters, E. Dinesh Pillai and M. A. Duncan, Solvation Dynamics in $Ni^{+}(H_2O)_n$ Clusters Probed with Infrared Spectroscopy, *J. Am. Chem. Soc.*, 2005, **127**, 16599–16610.